Geodesic, Flow Front and Voronoi Diagram

C. K. Au

Nanynag Technological University, mckau@ntu.edu.sg

ABSTRACT

Geodesics and flow fronts are orthogonal to each other. These two sets constitute the space time function of a source and play an important role in dealing with two types of problem: initial value problem and final value problem. This paper reveals the computation of the flow fronts from a point source in a two dimensional domain with a given velocity field. A space time function is established for the point source. The space time functions of the higher dimension sources such as line source, curve source and polygonal source can be derived geometrically based on that of a point source. Co-operation and competition between two sources in a two dimensional domain and their relationship with Voronoi diagram is presented.

1. INTRODUCTION

Orthogonal to the direction of the flow is the so-called flow front – these are terms come from fluids dynamics. Indeed, the transport of matter or energy is fundamental to thermal and fluid studies. But "flow" and "front" are not unique to these areas. An orthogonal set such as the normal and the tangent also arises in optics. There, the pair is called ray and wave front, respectively. Actually, the roots of the orthogonal pair date back several hundred years. Perhaps taking a hint from Fermat, Bernoulli blended mechanics with optics in the celebrated formulation of the Brachistochrone (or least time) problem. As science matures, the orthogonal set of the shortest path and the Hamilton-Jacobi characteristic surface, arising from theoretical mechanics, are now firmly embraced by optimization, as well as by control theory. As geometry is related to mechanics, it should not be surprising that there are counterparts in differential geometry; they are called: geodesic and isosurface. Table 1 summarizes the seemingly disparate fields and the terms; those in *italics* are adopted in this paper.

Thermal/fluids	Optics	mechanics/optimization/control	geometry
flow	Ray	shortest path	*geodesic*
flow front	wave front	Hamilton-Jacobi surface	Iso-surface
	(or eikonal)		(or iso-curve)

Tab. 1: Orthogonal Sets.

The mathematical details and properties of the geodesics can be found in the reference 1. Most of the researches in geodesics concentrate on various methods to compute the curve for a given surface which is either analytical[2], parametric[3] or discrete[4-8]. Other generates a surface pencil from a given geodesic[9]. The geometric aspects of a geodesic are explored in these works. This article addresses the computation of a geodesic from the view of its physical meaning. It begins by stating the problem that the calculus of variations solves: find a path between two points, which minimizes the time function, in a domain with a given velocity field. Using two velocity fields, $v = k$ and $v = ky$ (where k is a constant). Based on the geodesics, the flow fronts from a point source can be derived. Two phenomena, co-operation and competition of having more than one source in a domain are discussed. The filling pattern prediction in plastic injection moulded part is discussed as an application example.

2. GEODESICS, POINT SOURCE AND FLOW FRONT

A *geodesic* is the minimal path between two points. The spatial coordinates will be denoted by (x, y) Given a path parametrized in u, with components $x(u)$ and $y(u)$, its *line element* $(ds)^2 = (dx)^2 + (dy)^2$ is invariant. As it will be useful, the conversion factor between the parameter u and the arc length s is $ds = \sqrt{(x_u)^2 + (y_u)^2}\,du$ where $x_u = \frac{dx}{du}$

and $y_u = \frac{dy}{du}$. The time to travel along a path γ with velocity v is given as $t = \int_{\gamma_\theta} \frac{ds}{v}$. The calculus of variation allows one obtain a differential equation for describing the path that minimizes the time of travel between two points which is a geodesic in the form of

$$\frac{\partial \eta}{\partial x} = \frac{d}{ds}\left(\eta \frac{dx}{ds}\right) \tag{1.1}$$

$$\frac{\partial \eta}{\partial y} = \frac{d}{ds}\left(\eta \frac{dy}{ds}\right) \tag{1.2}$$

where $\eta = \frac{1}{v}$.

Since the left hand side of equation (1.1) and (1.2) involves the Euclidean coordinates and its right hand side is the arc length, it may be referred to as the *spatial* form of a geodesic. The geometry of a geodesic between two points depends upon the *velocity field* v within a domain.

A *point source* **j** in a domain **D** is characterized by two parameters: emission velocity v_j and the instant it starts emission t_j with respect to a reference time $t = 0$. Based on the principle of least action, the path γ_θ from source **j** at the instant t_j to a point **q** at time t in a domain **D** with velocity field v is a geodesic governing by the equation $t = t_j + \int_{\gamma_\theta} \frac{ds}{v}$.

The flow front from an emitted point source **j** is the front line of the emission. It is a topological circle in the domain D. An advancing flow front is a function of time t. The flow front possesses the geometrical property that it must be *orthogonal* to the geodesic from the source, hence, the equation of the flow front at time t is given by

$$t - \left(t_j + \int_{\gamma_\theta} \frac{ds}{v}\right) = 0\,,\ \forall \theta \in [0, 2\pi] \tag{2}$$

For instance, in a domain **D** with a *constant* velocity field, the geodesic from a point (x_0, y_0) takes on the form of a *straight line*. Let the location of a source **j** be (0,0). The geodesic from **j** to **q** is $\begin{bmatrix} x \\ y \end{bmatrix} = \begin{bmatrix} vt\sin\theta \\ vt\cos\theta \end{bmatrix}$ where v is the velocity. Therefore, the flow front is expressed as $t - \frac{\sqrt{x^2 + y^2}}{v} = 0$ (with $t_j = 0$), which is a family of concentric circles with variable t. Figure 1 shows the geodesics and the flow fronts from a source **j** with constant emission velocity.

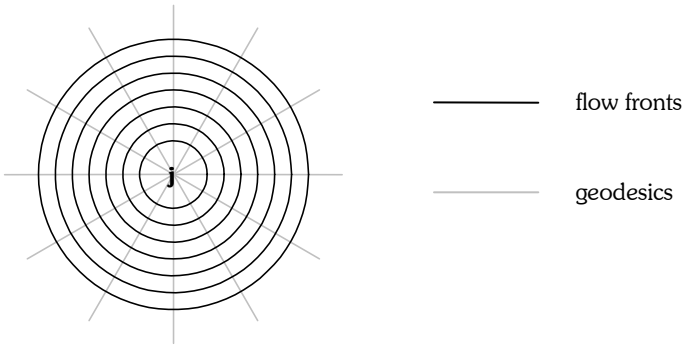

Fig. 1: Flow fronts of a point source **j** with constant velocity.

3. SPACE TIME FUNCTION OF A SOURCE

A *space time* describes the position in domain **D** with a velocity field v at a specific time instant. The equation of flow front,

$$t - \Psi(x, y) = 0 \tag{3}$$

with $\Psi(x, y) = t_j + \int_{\gamma_\theta} \frac{ds}{v}$ gives the relationship between a two dimensional space (in terms of x, y) and time. Hence, the space time function of a point source **j** at $(0, y_0)$ in a velocity field $v = k$ (where k is a constant) is $t - \left(t_j + \frac{\sqrt{x^2 + (y - y_0)^2}}{k} \right) = 0$, where t_j is the time delay of source **j**.

Figure 2 shows space time function of a point source **j** at $(0, y_0)$ in a constant velocity field with a time delay t_j. The black curves link all the *events* happen simultaneously while the grey lines are the *world lines*. Projecting these black and grey curves onto the space (xy plane) gives the flow fronts and the geodesics in the domain D.

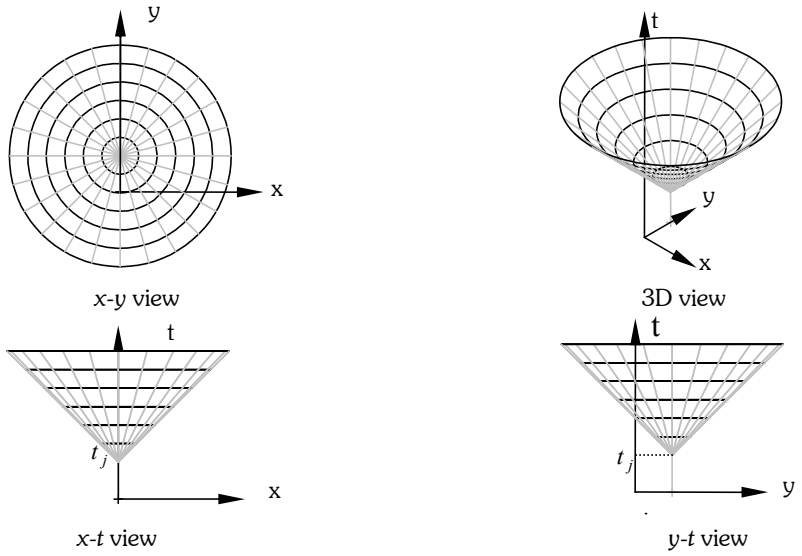

Fig. 2: Space time function of a point source in a constant velocity field.

When there exit more than one source in a domain, two possible phenomena arise:

1. these agents *co-operate* to acquire territories and;
2. these agents *counteract* to compete for territories.

Let $t = \Psi_{\mathbf{j}}(x, y)$ and $t = \Psi_{\mathbf{k}}(x, y)$ be the space time functions for two sources **j** and **k** in a domain **D**. The resultant space time function is:

$$t = \min[\Psi_j(x, y), \Psi_k(x, y)], \forall (x, y) \in \mathbf{D} \tag{4}$$

If these agents co-operate, then the resultant flow front at time t is given by the Boolean union of the function $\Psi_j(x, y) \bigcup \Psi_k(x, y)$.

For instance, a curve source is a typical example of co-operation. A curve source **c** in a domain **D** can be considered as an aggregation of infinite number of point sources along the curve. All these point sources co-operate to acquire territories. The flow front of the curve source at time t is $\bigcup_j \Psi_j(x, y)$, $\forall \mathbf{j} \in \mathbf{c}, \forall (x, y) \in \mathbf{D}$. Hence, the space time

function of a curve source is the envelope obtained by sweeping the space time function of a point source with time delays. Figure 3(a) and 3(b) show the space time functions of a line and a curve source with various time delay in a domain with a constant velocity field respectively. Similarly, the space time function of a polygonal source in a domain with constant velocity field is shown in figure 3(c).

(a) line source with variable time delay in a constant velocity field

(b) curve source with constant time delay in a constant velocity field

(c) polygonal source with constant time delay in a constant velocity field

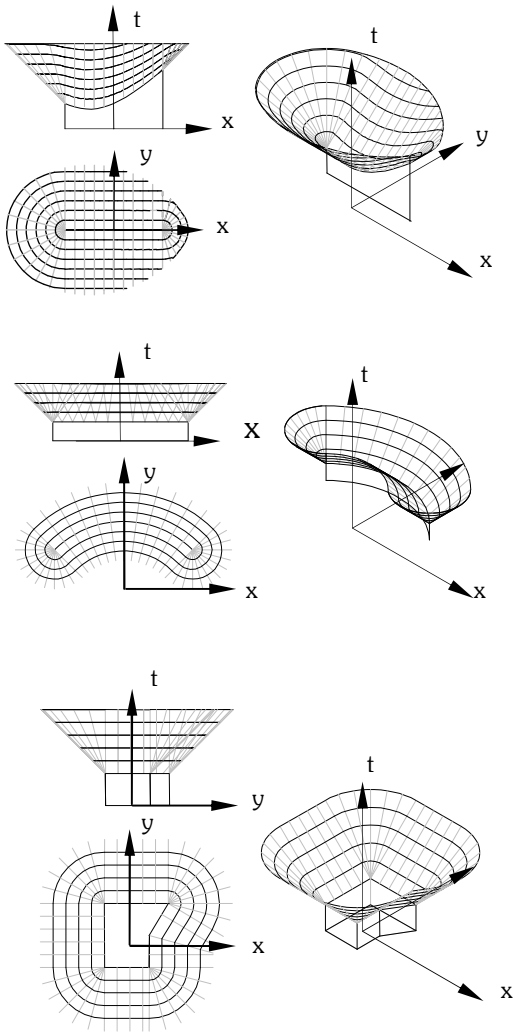

Fig. 3: Various curve sources.

If the agents counteract and compete for territories, a frontier μ exists to partition the domain. This frontier is the *algebraic intersection* of their space time functions. Therefore,

$$\mu_{j,k}(x,y,t) = \left\{(x,y,t) \mid \left(t = \Psi_j(x,y)\right) \bigcap \left(t = \Psi_k(x,y)\right)\right\} \quad (5)$$

Voronoi diagram in computational geometry demonstrates this phenomenon.

4. VORONOI DIAGRAM

A Voronoi diagram partitions the space based on a set of given sites according to a membership function. A distance function measuring the Euclidean distance is commonly employed. Such a distance function assumes a constant velocity field on the Euclidean space. Considering each sites as a source, the flow front propagates along the geodesic from the sources. A Voronoi diagram can be generated by projecting the space time function on the space as shown in figure 4.

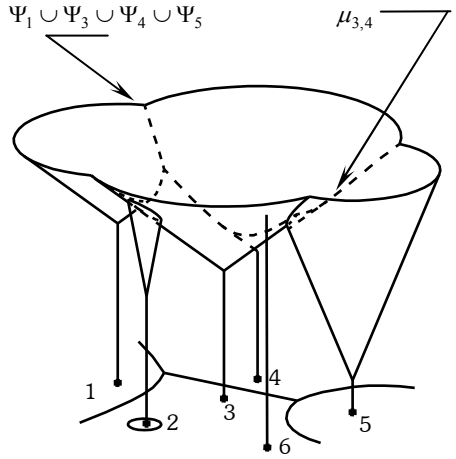

Site	Characteristics (t_j, v_j)
1	(12.5,1.732)
2	(10,0.268)
3	(10,1.732)
4	(10,1.732)
5	(2.5,0.577)
6	(20,0.268)

Fig. 4: A Voronoi diagram.

Hence, it can be seen that the flow front is the boundary of the growing space time function while the frontier is the internal edges. This information is obtained by modeling the space time function as solid geometry and performing the Boolean operation "union". An algorithm for constructing a Voronoi diagram with varies site characteristics based on solid modeling is listed in figure 5:

```
create a solid geometry K_0 based on t_0 and v_0 at q_0
while (not done) do
begin
    create a solid geometry K_j based on t_j and v_j at q_j
    K_0 ← K_0 ∪ K_j
end
extracting the edges in K_0
projecting the edges onto the domain
```

Fig. 5: An algorithm for constructing the Voronoi diagram.

Figure 6 shows a Voronoi diagram for sites with various dimensionalities. Site **1** and **2** are point sites (source), site **3** is a line site (source) while site **4** is a polygonal site (source). Their space time functions are depicted in figure 3. These sites possess different site characteristics.

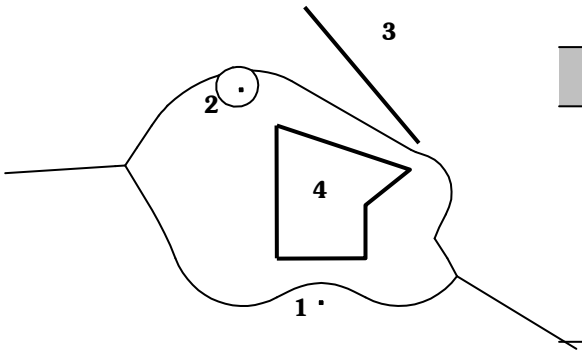

Sites	Site characteristics (t_j, v_j)
1	(3.25, 1.73)
2	(1.25, 0.27)
3	(2.50, 1.73)
4	(2.50, 1.00)

Fig. 6: A Voronoi diagram for sites with various dimensionalities.

However, these agents usually co-operate to acquire territories and counteract internally *simultaneously*. Hence, the combination of the two phenomena usually arises. The filling of the injection moulding is an example to illustrate this situation. The melt flow in the cavity is split due to the changes in flow velocity. These split flows are co-operating to earn the territory (to fill up the cavity) and competing individually so that weld lines exist.

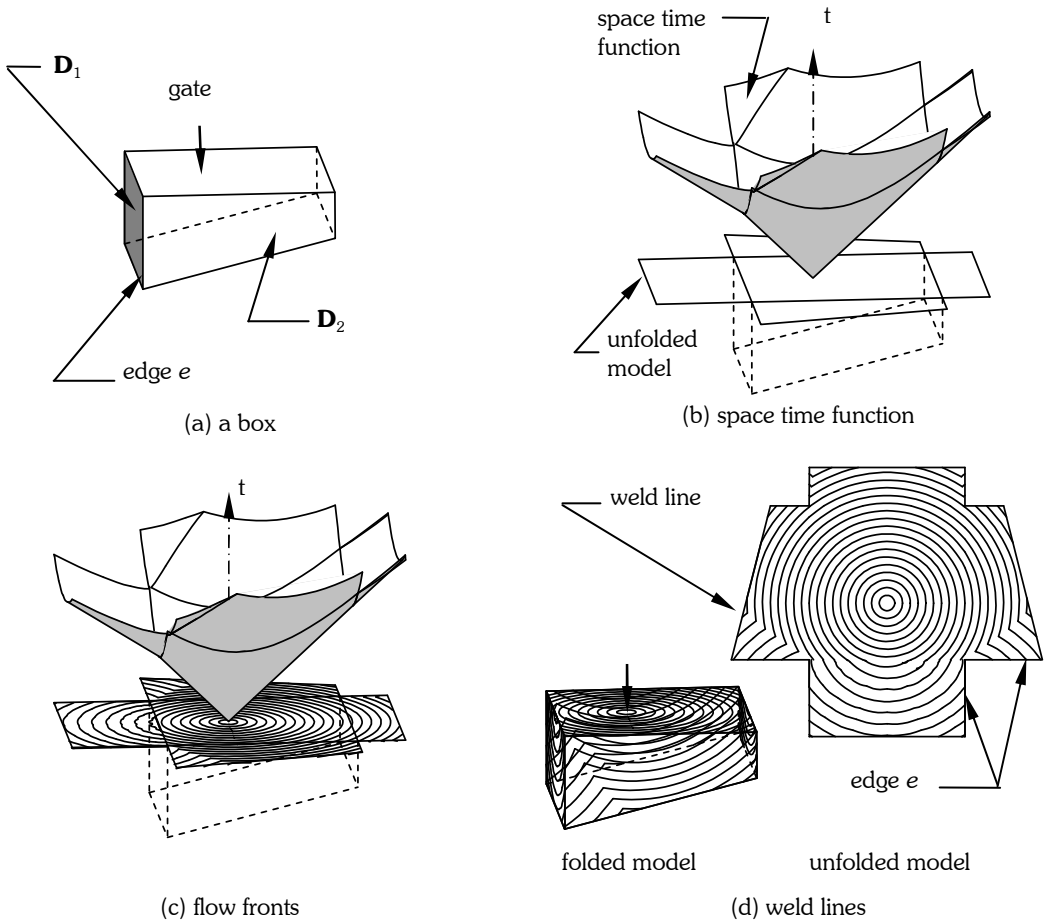

Fig. 7: Filling simulation of a molding.

Figure 7(a) shows a moulding with two different wall thicknesses. The thickness of domain $\mathbf{D}_1$ is greater than that of $\mathbf{D}_2$. Melt flows into the cavity from the gate (a point source) with constant velocity. For simplicity, the flow velocity is assumed to be directly proportional to the wall thickness. The edge *e* is common to both domains $\mathbf{D}_1$ and $\mathbf{D}_2$ and the velocity in $\mathbf{D}_1$ is faster. Hence, *e* is a line source in domain $\mathbf{D}_2$. The space time function is shown in figure 7(b) with the model unfolded. Sectioning this function and projecting onto the unfolded model yields the flow fronts as depicted in figure 7(c). A discontinuity in the space time function indicates a weld line. Figure 7(d) gives the flow fronts and weld lines for both folded and unfolded model.

Figure 8(a) gives a flow front pattern generated by finite element method with detail calculation of the flow velocity (instead of assuming it as a constant) while the flow front pattern in figure 8(b) of the same molding is obtained by the kinetic source approach. It can be seen that both patterns are basically agreeable, particularly the location of the weld line.

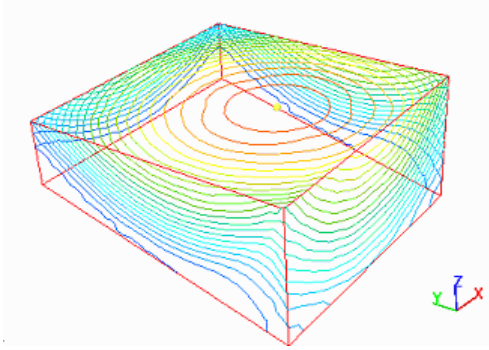

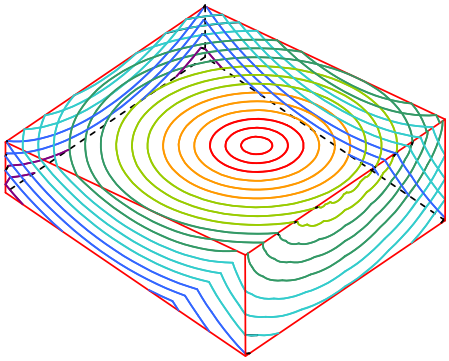

(a) flow fronts generated by finite element method (b) flow fronts generated by kinetic source approach

Fig. 8: Flow fronts.

5. CONCLUSION

From Minkowski to Einstein[12], space and time are not separated. Hence, a minimal path in time between two points in the space is the geodesic between two events in the space time. The space time function plays an important role in solving two types of problem: *initial value problem* and *boundary value problem*. The initial value problem refers to the computation of the geodesic in space time for a given initial conditions: initial position, velocity and incident angle while the boundary value problem computes the geodesic between two events in the space time.

Geodesics, flow fronts and space time functions are discussed in this article. Based on the space time function of a point source, space time functions of the higher dimension source such as curve and polygonal source can be obtained. Hence, the flow fronts of a curve source and a polygonal source is generated by slicing the space time function and projecting on the domain. While geodesics between two points in the domain are derived since geodesics and flow fronts are orthogonal set.

The space time functions of multiple sources describe the three phenomena: co-operation between two agents, competition between two agents, and the combination of these two phenomena.

An approach for spatial partitioning and constructing filling patterns for laminar flow simulation with some known velocity fields are demonstrated.

6. REFERENCES

[1] Do Carmo, M. P.: Differential Geometry of Curves and Surfaces. Prentice-Hall, Englewood Cliffs, NJ. 1976

[2] Patrikalakis, N. M.; Badris, L.: Offsets of Curves on Rational B-spline Surfaces, Engineering with Computers 5, 1989, 39-46.

[3] Spivak, M.: A Comprehensive Introduction to Differential Geometry. 2nd ed. Houston. 1979.

[4] Kimmel, R.; Sethian J. A.: Computing Geodesic Paths on Manifolds, Proceedings of National Academy of Sciences, 95(15), 1998, 8431-8435.

[5] Kimmel, R.; Kiryati, N.; Bruckstein, A. M.: Multi-valued Distance Maps in Finding Shortest Paths Between Moving Obstacles, IEEE Trans. Robot Automation, 14(3), 1998, 427-436.

[6] Novotni, M.; Klein, R.: Computing Geodesic Paths on Triangular Meshes, Proceedings of The 10-th International Conference in Central Europe on Computer Graphics, Visualization and Computer Vision'2002 (WSCG'2002). 2002.

[7] Polthier, K.; Schmies, M.: Straightest geodesics on polygonal surfaces. In: Hege, H. C.; Polthier, K. editors. Mathematical Visualization, Berlin: Springer. 1998.

[8] Ravi Kumar, G. V. V.; Srinivasan P.; Devaraja Holla, V.; Shastry, K. G.: Geodesic curve computations on surfaces, Computer Aided Geometric Design, 20(2), 2003, 119-133.

[9] Wang, G.; Tang, K.; Tai, C.: Parametric representation of a surface pencil with a common spatial geodesic, Computer-Aided Design, 36(5), 2004, 447-459.

[10] Stahl, S.: The Poincare half plane, Jones and Bartlett Publishers, 1993.

[11] Okabe, A.; Boots B.; Sugihara, K.: Spatial Tessellations: Concepts and Applications of Voronoi Diagrams, John Wiley & Sons, New York, 1992.
[12] http://physics.syr.edu/courses/modules/LIGHTCONE/minkowski.html